Vol. 47, No. 2 (2025) 279-293, DOI: 10.24874/ti.1841.12.24.03

Tribology in Industry

www.tribology.rs

RESEARCH

Taguchi Method for Tribological Excellence: Insights into Copper-Based Metal Matrix Composites

S.S. Kallesh[a,*], Rajaneesh N. Marigoudar[b]

[a]*Department of Mechanical Engineering, Smt. Kamala and Sri Venkappa M. Agadi College of Engineering and Technology (affiliated to VTU, Belagavi), Lakshmeshwara, India,*
[b]*Department of Mechanical Engineering, Jain Institute of Technology, Davangere, India.*

Keywords:

Copper-SiC composites
Powder metallurgy
Microstructure
Hardness
Wear
Taguchi technique
Scanning electron microscope

* Corresponding author:

S.S. Kallesh
E-mail: sskallesha@gmail.com

Received: 26 December 2024
Revised: 1 February 2025
Accepted: 27 March 2025

A B S T R A C T

Copper matrix composites are widely used in brakes and bearings due to their excellent mechanical properties, wear resistance, and thermal management. This study examines the dry sliding wear of copper matrix composites reinforced with silicon carbide (SiC) particles, produced via powder metallurgy. Optimization of the tribological behavior was conducted via the Taguchi technique and ANOVA were used to analyze wear loss. Confirmation tests were conducted to validate the experimental results. Examined samples were analyzed using a scanning electron microscope. Regression model for predicting wear loss was developed using the Taguchi technique. The influence of SiC loading and tribo-parameters, including applied load, sliding speed, and sliding distance, on the dry sliding wear of the composites was examined using L_{27} orthogonal array. Microstructural analysis and hardness data revealed a uniform distribution of SiC particles within the copper matrix, with composite hardness increasing as SiC loading increased. The greatest influence on wear loss was the wt. % of SiC (29.33 %), followed by sliding speed (27.53 %) and applied load (20.66 %), while sliding distance had the least impact (19.32 %). Increasing SiC from 5 to 10 wt. % reduced wear loss by 15.73 %, whereas an increase from 10 to 15 wt. % led to a 9.33 % reduction. The results obtained in this study using the Taguchi technique are valuable for enhancing and further exploring the friction and wear behavior of hybrid particulate-reinforced copper matrix composites.

1. INTRODUCTION

Much research is being done on the development and enhancement of composite materials to improve material performance in tribological applications. Copper matrix composites (Cu-MMCs), have attracted a lot of interest because of their exceptional thermal conductivity, wear resistance, and mechanical strength. However, achieving an optimal balance of these properties necessitates a systematic and reliable approach to material design and process

optimization. Among Cu-MMCs, composites reinforced with ceramic particles have emerged as highly promising engineering materials. Cu-MMCs are ideal for applications like electrical contact materials, resistance electrodes, and other industrial uses because they have superior wear resistance, microstructural stability, and high-temperature performance when compared to Cu and Cu alloys [1–5].

Pure Cu has exceptional conductivity, but its mechanical characteristics deteriorate dramatically at high temperatures, which restrict its use in these environments [6-8]. One effective method to overcome this limitation is to include ceramic particles into the Cu matrix. This process maintains Cu's remarkable electrical and thermal conductivity, raising the material's potential applications while also enhancing its mechanical strength and wear resistance [9,10]. Due to their high thermal stability, ceramic particles such as oxides, borides, and carbides are well-suited for this purpose. Consequently, they have been used to reinforce Cu-MMCs, making them reliable electrode materials for demanding, high-temperature applications [11].

In engineering applications, MMCs have drawn lot of attention due to their enhanced mechanical properties, good thermal stability, and high specific strength [12-15]. The best option among the different reinforcements used to improve MMCs is silicon carbide (SiC). Ceramics made of SiC are renowned for their outstanding hardness and thermal stability. SiC improves the overall hardness, strength, and stiffness of MMCs when it is utilized as reinforcement. This is important for applications that require resistance to deformation and mechanical wear. Because of its natural high hardness, SiC particles greatly increase wear resistance when added to metal matrices [16-18]. This characteristic is particularly beneficial for industrial machinery exposed to high friction, as well as aerospace and automotive components like brake disks, clutches, and cylinder liners.

Shabani et al. [19] used sintering in conjunction with the application of compressive force to produce Cu/SiC composites. The study shows that adding SiC particles to the Cu matrix reduces porosity, increases density, and enhances wear resistance. Sinter-forging is particularly effective for producing high-performance Cu/SiC composites suited for applications requiring superior wear resistance. The wear behaviour of Cu and its composites made by hot isostatic pressing was investigated by Tjong and Lau [20]. According to the wear tests, Cu exhibited more wear loss than Cu containing 20 wt. % SiC particles. This was the outcome of the reinforcing SiC particles effectively reducing wear, and deformation in the subsurface region during sliding.

The Taguchi technique is a reliable method for process optimization and product quality improvement, systematically analyzing factor effects on desired outcomes [21,22]. It is extensively used in materials engineering, including for the analysis and optimization of MMCs' dry sliding wear. Sahin [23] conducted an experimental study using Taguchi technique to investigate the wear of Al2014 and Al2014/10 wt. % SiC composites with various SiC abrasive grits under varying tribo-test situations. The results indicate that the SiC loading had the greatest influence, making it the primary factor in two-body abrasive wear, followed by applied load. Parametric studies based on experimental design by Suresha et al. [24] show that hybrid composite (SiC+graphite) exhibit superior wear resistance compared to Al/SiC composites. Furthermore, wear is positively influenced by load and sliding distance, but speed has the opposite effect, decreasing wear as it rises. Table 1 summarizes recent research studies and key findings on the wear behavior of SiC-reinforced Cu composites fabricated using various processing methods. Micron-sized SiC improves wear resistance and increases the coefficient of friction, while the additions of nano-SiC reduces both friction and wear loss [25-30,31,32].

The review of existing literature indicates a scarcity of experimental studies investigating the influence of SiC loading and their varying wt. % on wear of Cu-MMCs produced via powder metallurgy technique. Hence, this work aims to explore the wear behaviour by SiC loading of 5, 10, and 15 wt. % into Cu matrix using Taguchi technique. Analysis of variance (ANOVA) will be used to quantify the percentage influence of various factors on composite wear. These composites are designed for automotive, marine, railroad, and aerospace applications.

Table 1. Recent research works related to wear behavior of SiC reinforced Cu composites.

Composite constituents	Processing method	Research highlights	Ref.
Cu-SiC	Friction stir processing	The impact of manufacturing parameters on wear properties is not well understood, making it challenging to predict composite behavior. The wear mechanisms in Cu-SiC composites are unclear, complicating the analysis of wear rates and debris formation.	[25]
Cu-SiC	Hot isostatic pressing	20 vol.% SiC composite shows lower wear loss than pure copper.	[26]
SiC/Cu modified by SiO_2–Cu_2O glass phase	Sol-gel method and hot pressing sintering.	The 5 vol. % glass phase exhibited high microhardness (149 ± 2.3 HV), the lowest friction coefficient (0.34 ± 0.02), and an average wear rate of 1.12×10^{-5} ± 0.09 mm^3/N m.	[27]
Cu–SiC nanocomposites	High-pressure torsion	The produced composite material showed a reduced coefficient of friction and high wear resistance.	[28]
Cu–SiC foam	Template method combined with reaction sintering	SiC foam ceramic enhances Cu alloy and friction components through its 3D structure. These composites exhibit high-temperature resistance, low wear rate, and stable friction coefficient.	[29]
Cu-SiC	Powder metallurgy	Tribological capabilities can be enhanced by optimizing factors like SiC reinforcement, surface modification, consolidation process, and wear conditions.	[30]
SiC/Cu nano-composite	Powder metallurgy	Increasing SiC nanoparticles reduced the copper matrix grain structure and improved wet wear resistance.	[31]
Particulate reinforced Cu-based composites	Different methods	Cu-MMCs show enhanced mechanical strength, wear resistance, and self-lubrication due to ceramic and SL reinforcements. Protective transfer layers and SLs reduce direct contact, promoting smoother interactions between surfaces.	[32]

2. MATERIALS AND METHODS

2.1 Materials

High-purity (99.9 %) electrolytic copper (Cu) powder with a size < 60 μm is supplied by M/s. Parashwamani Metals, Mumbai, India, as the matrix material. The silicon carbide (SiC) was purchased from Carborundum Universal Ltd, Chennai, India, and has an average particle size of 15–25 μm. Tables 2 and 3, respectively, list the characteristics of Cu and SiC particles.

Table 2. Properties of copper powder.

Properties	Cu powder
Appearance	Reddish
Crystal structure	Cubic, Face Centered
Coeff. of thermal expansion	16.4×10^{-6}/°C
Density	8.96 g/cm^3

Table 3. Properties of silicon carbide powder.

Properties	SiC powder
Appearance	Black grey
Coefficient of thermal expansion	4.0 x10^{-6}/°C
Thermal conductivity	120 W/m•K
Density	3.16 g/cm^3
Mohs hardness (New scale)	13
Fracture Toughness	6.85 MPa $m^{0.5}$

2.2 Fabrication using powder metallurgy technique

In this study, Cu/SiC composites were processed using the powder metallurgy technique as depicted in Figure 1. In a ball mill, Cu powder was mixed with 5, 10, and 15 wt. % SiC powder for 8 h to produce the mixed powders. A hydraulic compacting press was used to apply uniaxial pressing to blended metal powders, cold compacting them for 10 min at 70 kN to produce a high-density composites. Mixed metal powders are heated below its melting point under regulated atmospheric pressure to enable material bonding. The mixed electrolytic Cu powder was sintered to enhance its mechanical properties. The compressed green pellets were then sintered for 7 h at 700 °C in a tubular sintering furnace with an argon atmosphere present, at heating rate of 12 °C/min. The prepared Cu and Cu/SiC composite samples are depicted in Figure 1. Sintering furnace specifications are as follows: Make: Lakshmi Vacuum Technologies, Bangalore; Product capacity: 15 to 50 kg per charge; Sintering temperature: 650-1200 °C; Soaking dimensions: 150 mm × 140 mm × 350 mm; Vacuum tank: Ø

600 mm × 800 mm; Temperature rise time: Up to 1500 °C. Table 4 displays the developed composite samples and compositional specifications.

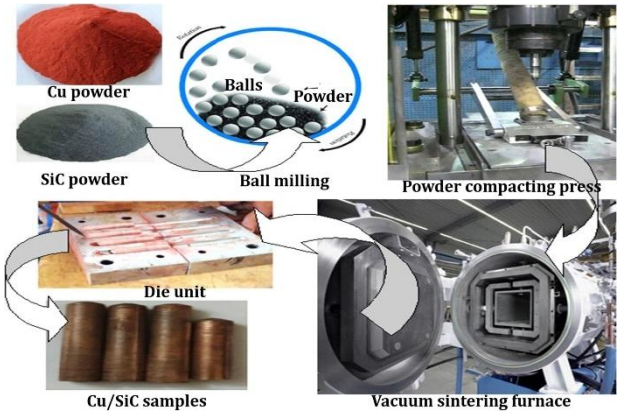

Fig. 1. Processing of Cu/SiC composites by powder metallurgy technique.

Table 4. Composition of Cu/SiC composites.

Composites	Copper (wt. %)	SiC (wt. %)
Cu	100	---
Cu/5SiC	95	5
Cu/10SiC	90	10
Cu/15SiC	85	15

2.3 Density test

The density of Cu and Cu/SiC composites was determined using Archimedes' principle. This technique involves measuring the difference in the specimen's weight in air compared to its weight when suspended in distilled water at room temperature. Subsequently, the porosity of samples was calculated using the porosity (P) equation (1):

$$P = 1 - \frac{\rho_t}{\rho_m} \quad (1)$$

where, ρ_t = theoretical density of the composite, ρ_m = measured density of the composite.

2.4 Microstructure and hardness test

In order to achieve the best mechanical properties in MMCs, the microstructure must be precisely controlled using powder metallurgy. The microstructure of the Cu and Cu/SiC composite samples was investigated. The samples cut from the slabs were polished to a mirror finish. A Joel JSM-6510LV SEM was used to examine the bonding interface among the SiC particles and Cu matrix.

Copper and Cu/SiC composites were subjected to microhardness tests using ASTM E18-24 standards and a 1/16 mm steel ball weighing 1000 N [33]. For the test, samples with size of 15 mm in length and 8 mm diameter were prepared using wire EDM machine. To minimize errors, six sets of readings have been taken on the composite surface at various locations.

2.5 Dry sliding wear test

A Pin-on-Disk wear tester as shown in Figure 2 (Magnum Engineers, Bangalore, India) was utilized to carry out sliding wear test of Cu and Cu/SiC composites in compliance with ASTM G99-23 standards [34]. Wear tester specifications are as follows: Normal load range: Up to 200 N; Frictional force range: Up to 200 N (1 N resolution); Wear measurement range: ± 2 mm with tare function; Disc speed: 100 to 2000 rpm; Wear disc diameter: 165 mm × 8 mm thickness; Wear disc track diameter: 10 to 140 mm; Specimen pin diameter/diagonal: 3 mm to 12 mm; Pin length: 10 to 25 mm. Heat-treated EN32 steel disk with a surface hardness of 65 HRC serves as the counterface. A 0.15 µm polish was applied to the surface. Cu/SiC composites and Cu were used to produce cylindrical pins that were 8 mm diameter and 15 mm height. To make sure the samples made full contact and stood upright with the counterface, they were ground and polished using 1500 grit SiC abrasive paper. Prior to testing, the polished specimens were weighed and meticulously cleaned using ethanol.

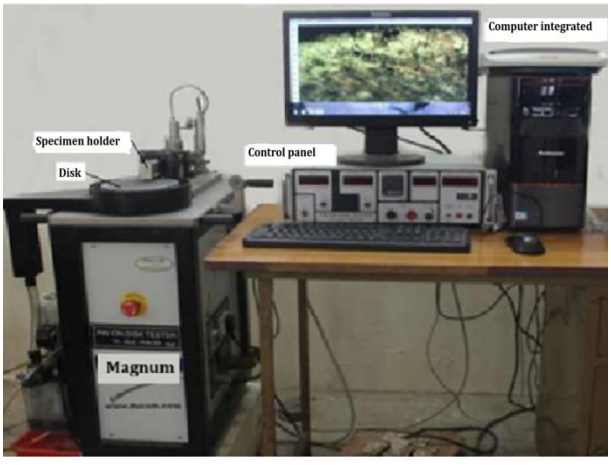

Fig. 2. Pin-on-Disk wear tester.

Figure 3a–d presents the Cu and Cu/SiC composite wear test samples before and after test. Figure 3a shows the wear test samples before and after the test, while Figures 3b–d depicts Cu matrix composites with varying SiC content.

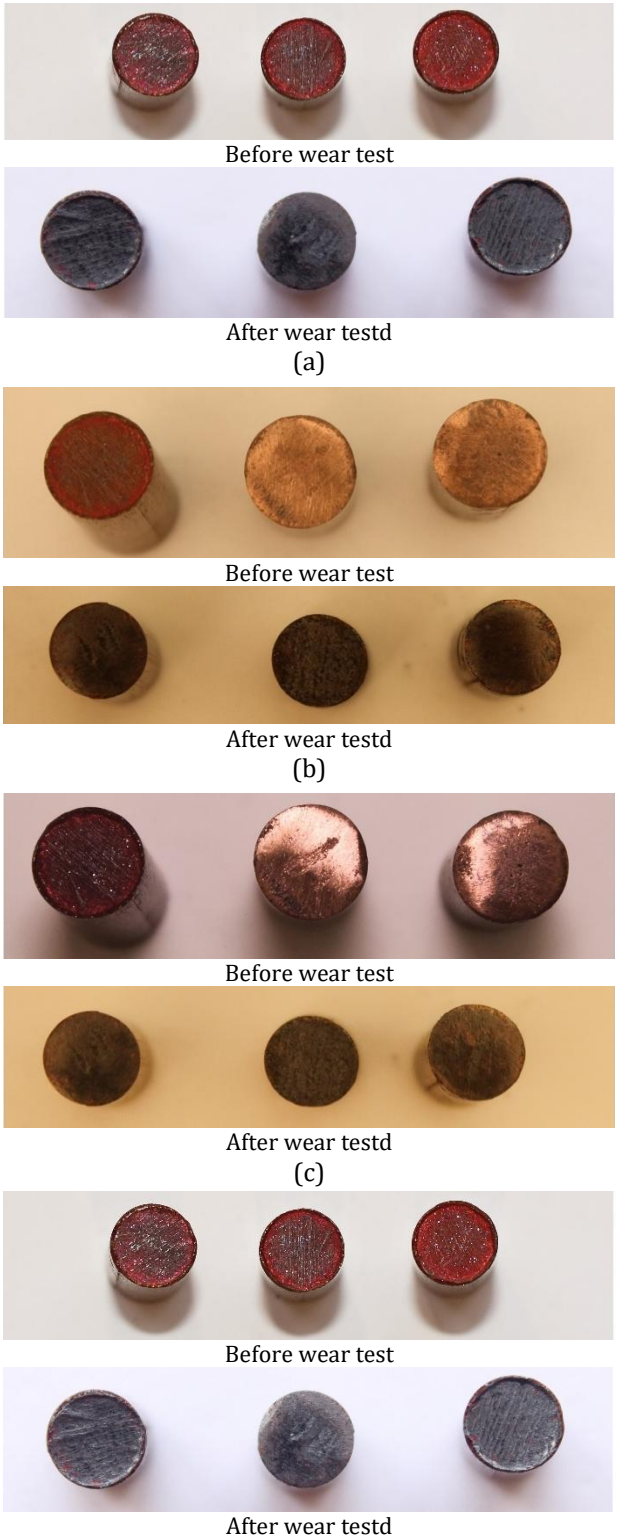

Fig. 3. Composite wear test samples before and after test: (a) Cu, (b) Cu/5SiC, (c) Cu/10SiC, (d) Cu/15SiC.

Wear test parameters were specified in Table 5. Three test results were averaged to calculate the weight loss. A high-precision analytical weighing scale with an accuracy of 0.1 mg was used to determine the samples' initial and final weights. Taguchi designed experiments to determine the influence of SiC wt. % (A), applied load (B), sliding speed (C), and sliding distance (D) on the wear loss of the composites. To investigate the significance and contribution percentage of the tribo-parameters, as well as ANOVA was performed.

Table 5. Control factors and levels.

Control factors	Levels		
	1	2	3
SiC loading (wt. %)	5	10	15
Applied load (N)	10	20	30
Sliding speed (RPM)	200	400	600
Sliding distance (km)	1	2	3

After the wear test, the worn-out surfaces of the chosen Cu and Cu/SiC composites were inspected under a scanning electron microscope (SEM; JEOL, model JSM-6510LV) to identify the involved wear mechanisms.

2.6 Wear analysis by design of experiments

Many industries use Taguchi technique, a conservative and efficient optimization technique, for multiple sample comparisons. Orthogonal arrays, which find the ideal control process parameter settings with a small number of tests, make it possible to design high-quality systems. Signal-to-Noise (SN) ratios, which are typically classified as nominal-the-better, higher-the-better, or lower-the-better, are calculated from test results.

To reduce wear loss, the SN ratio in this study was determined using the smaller-the-better criterion. Equation (2) [22] illustrates how the SN ratio is computed as a logarithmic transformation of the loss function.

$$\frac{S}{N_B} = 10\log\left(\frac{1}{n}\sum_{i=1}^{n} y_i^2\right) \quad (2)$$

In equation (2), y = number of observations and n = observed data. Table 5 lists the four control factors that were measured at three different levels: sliding distance, sliding speed, applied load, and wt. % of SiC. The Minitab software receives these parameters along with their levels as input.

The Taguchi L_{27} orthogonal array was selected for this study based on the control factors and levels, and the tests were conducted accordingly.

3. RESULTS AND DISCUSSION

3.1 Density and porosity

Table 6 shows that as the SiC content of composites increases, their density tends to decrease. This is because SiC particles have a substantially lower density than copper.

Table 6. Composition of Cu/SiC composites.

Composites	Theoretical Density (g cm^{-3})	Measured Density (g cm^{-3})	Porosity (%)
Cu	8.96	8.95	0.11
Cu/5SiC	8.18	8.11	0.86
Cu/10SiC	7.56	7.49	0.93
Cu/15SiC	7.02	6.95	1.00

Copper has a very low porosity of 0.11 %, with a measured density of 8.95 g/cm^3 compared to the theoretical density of 8.96 g/cm^3. The theoretical density for the Cu/5SiC composite drops to 8.18 g/cm^3. Whereas, measured density is 8.11 g/cm^3 yielding marginally higher porosity of 0.86 %. The measured density drops even more at 10 wt. % SiC loading, yielding a porosity of 0.93%. At 15 wt. % of SiC, the porosity rises to 1.0 %. A less dense phase (SiC) is introduced, as evidenced by the results, which show an increasing trend in porosity with higher SiC loading. Since SiC has a lower density than Cu and a larger wt. %, the overall density of the composite decreases as more SiC is added. Higher measured porosity could be the result of more void spaces caused by the greater mismatch in densities between the two phases (Cu and SiC).

3.2 Microstructure of Cu and Cu/SiC composites

The most important factor in producing consistent characteristics for discontinuously reinforced MMCs is the spreading of the reinforcement. The performance of the composites can be inferred from the microstructure. In this work, powder metallurgy technique was followed to prepare Cu, and different SiC loadings into Cu matrix composites.

Figure 4a, b depicts the SEM images of Cu and SiC particles. The chemical composition (by weight) determined via EDX closely approximates that of the Cu matrix, with 97.8 % Cu, 33.6 % O, and 8.9 % C. The weight percentages of silica (Si), carbon (C), oxygen (O), and magnesium (Mg) are 61.97 %, 30.07 %, 7.09 %, and 0.87 %, respectively, indicating the dominant presence of silicon and carbon species in the samples.

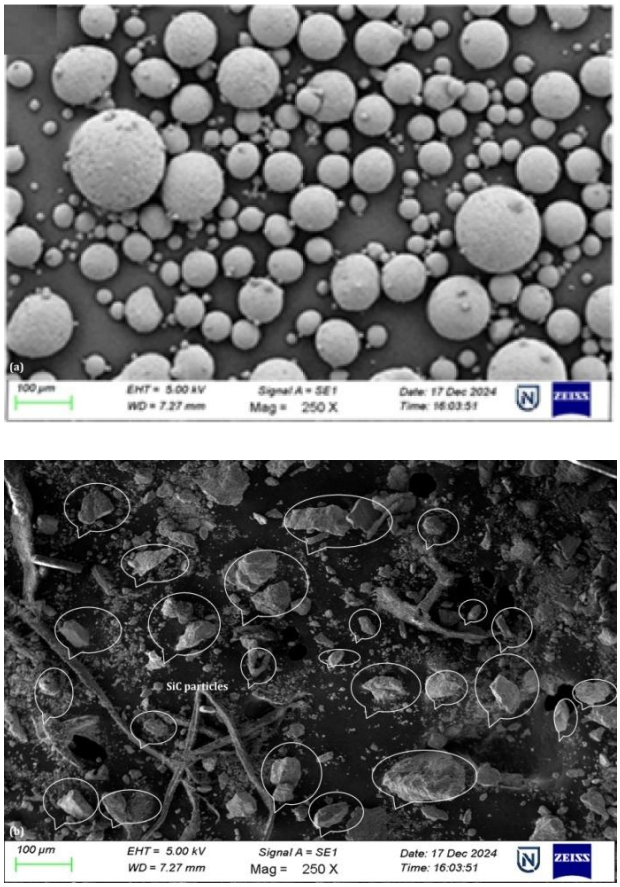

Fig. 4. SEM images: (a) Cu particles, (b) SiC particles.

Figure 5a-d displays the scanning electron microscopy (SEM) pictures of Cu and Cu/SiC samples. The SEM micrographs in Figure 5 reveal the distinct phases present in the Cu and Cu/SiC composites, with pure Cu (a) showing a uniform copper matrix, while the Cu/SiC composites (b, c, and d) display increasing amounts of SiC particles dispersed within the Cu matrix as the SiC content rises from 5 wt. % to 15 wt. %. A clear, dark matrix without reinforcing particles is seen in Cu (Fig. 5a). Figures 5b, 5c, and 5d show the morphology of 5, 10, and 15 wt. % SiC reinforced Cu composite samples, respectively. As reinforcement loading increases, more SiC particles are present.

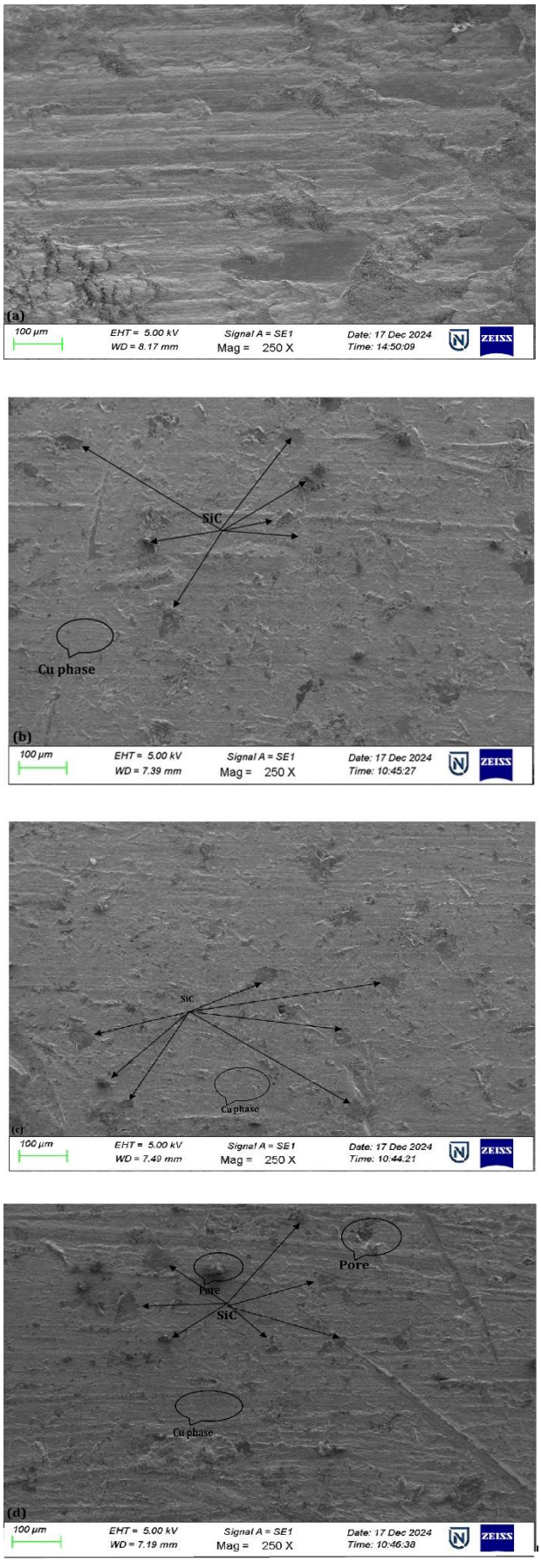

Fig. 5. Micrographs of Cu and Cu/SiC composites: (a) Cu, (b) Cu/5SiC, (c) Cu/10SiC, (d) Cu/15SiC.

Additionally, the Cu sample with 15 wt. % SiC exhibits superior reinforcement intensity. No area remains devoid of particle dispersion. Problems like grain boundary isolation are completely eliminated because sintering does not melt the Cu matrix material. Consequently, the distribution's nature can be regarded as homogeneous.

In order to improve wear performance in MMCs, it is essential that reinforcement be distributed properly, as this distribution type dominates all other microstructural characteristics [35]. Photomicrographs show that there is no particle drop-out during the metallographic preparation of the samples (Figs. 5c-d). This could suggest that there is good adhesion and bonding between the SiC particles and the Cu matrix. The Cu matrix of the composite seems to be continuous and devoid of other defects, such as large pores or voids. This observation guarantees proper consolidation of Cu and SiC particles during compaction and sintering.

3.3 Hardness

The hardness (HRB) of all Cu/SiC composite samples are higher than that of Cu, as Table 7 demonstrates, because SiC is hard owing to the covalent and ionic bonds [36].

Table 7. Hardness of Cu and SiC/Cu composites.

Composites	Hardness (HRB)
Cu	42 ± 1
Cu/5SiC	45 ± 2
Cu/10SiC	49 ± 1
Cu/15SiC	56 ± 2

Additionally, because of their more dense structure configuration and stronger interfacial bonding among the particles, all Cu/SiC composites have a higher hardness than Cu (SEM images, Figs. 5b-d). The soft matrix phase is apprehended in place by hard SiC particles, giving the composite its strength [37-40]. Furthermore, the soft Cu matrix is well-protected from dislocation by hard SiC particles. Due to a higher hardness value, the plastic flow is significantly impeded by an increasing SiC concentration in the Cu matrix.

3.4 Dry sliding wear behaviour

Table 8 summarizes the wear loss in grams (g) from wear tests that were performed for different wt. % of SiC (A), applied normal load (B), sliding speed (C), and sliding distance (D), according to L_{27} orthogonal array. The wear loss trend of Cu-reinforced SiC follows the order: Cu/5SiC > Cu/10SiC > Cu/15SiC composite samples. The shift in wear loss demonstrates that the wt. % of SiC in the Cu base material had a major influence on the wear trend.

Main effect plots for the SN ratios for wear loss in the composite samples are shown in Figure 6. According to the plot, the dominant effect is expressed by the parameter with the higher inclination. To figure out the significance and percentage of involvement of different factors, ANOVA was used.

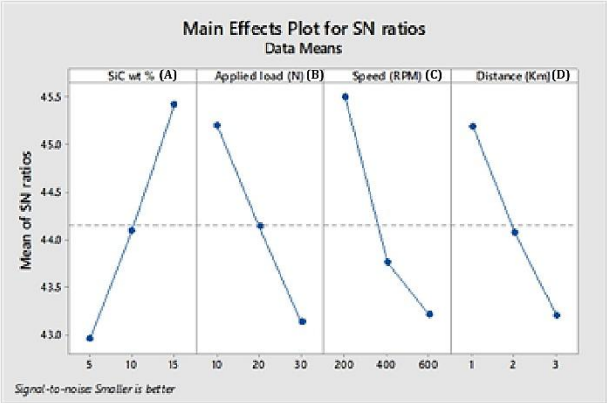

Fig. 6. Main effect graphs for S/N ratios.

The wear loss of all Cu/SiC composite samples are affected by the various tribological parameters including the SiC wt. % in the Cu composites as depicted in Figure 6. The influence of four factors namely (A) wt. % SiC, (B) applied load, (C) sliding speed, and (D) sliding distance; on the SN ratio is depicted in the 'Main Effects graph for SN Ratios' (Fig. 6). A smaller ratio is better for minimizing the wear loss.

Table 8. Testing according to L_{27} OA, and wear loss values in conjunction with their SN ratios.

Sl. No.	SiC wt. % (A)	Applied load N (B)	Speed RPM (C)	Sliding distance Km (D)	weight loss (g)	SN Ratio- (dB)
1	5	10	200	1	0.0049	46.196
2	5	10	400	2	0.0068	43.349
3	5	10	600	3	0.0079	42.047
4	5	20	200	2	0.0062	44.152
5	5	20	400	3	0.0079	42.047
6	5	20	600	1	0.0069	43.223
7	5	30	200	3	0.0075	42.498
8	5	30	400	1	0.0079	42.047
9	5	30	600	2	0.0089	41.012
10	10	10	200	1	0.0041	47.744
11	10	10	400	2	0.0057	44.88
12	10	10	600	3	0.0069	43.223
13	10	20	200	2	0.0056	45.036
14	10	20	400	3	0.0071	42.974
15	10	20	600	1	0.0062	44.152
16	10	30	200	3	0.0068	43.349
17	10	30	400	1	0.0071	42.974
18	10	30	600	2	0.0075	42.498
19	15	10	200	1	0.0034	49.370
20	15	10	400	2	0.0051	45.840
21	15	10	600	3	0.0062	44.152
22	15	20	200	2	0.0047	46.558
23	15	20	400	3	0.0064	43.870
24	15	20	600	1	0.0055	45.192
25	15	30	200	3	0.0059	44.582
26	15	30	400	1	0.0051	45.848
27	15	30	600	2	0.0068	43.349

Each factor influences the SN ratios in the ways listed as follows. The SN ratio improves dramatically (higher value) as the material composition rises from 5 % to 15 % wt. % SiC. An increase in SiC from 5 to 10 wt. % resulted in a 15.73 % decrease in wear loss. In contrast, there was a 9.33 % decrease in wear loss when SiC was raised from 10 to 15 wt. %. SiC is a hard ceramic material with exceptional resistance to abrasion and wear. SiC functions as a reinforcing phase when added to a matrix, assisting in the more efficient distribution of applied stress. The presence of SiC in the composite material increases its hardness, which minimizes deformation under frictional forces and decreases the depth of wear tracks. Figure 6 thus makes it clear that the major factor is parameter ((A); i.e., wt. % of SiC). The wear loss is decreased by higher SiC loading, most likely as a result of the SiC particles' increased hardness as indicated in Table 7, and wear resistance. In the present work, the SiC loading increases with the hardness of the Cu matrix material.

The SN ratio decreased with increase in the applied normal load from 10 N to 30 N. This suggests that greater loads result in increased wear loss because the increased contact pressure probably speeds up material removal.

Increasing the sliding speed from 200 rpm to 600 rpm, results in a decrease in the SN ratio. Thus, greater wear loss results from higher sliding speeds, most likely as a result of higher frictional heat and mechanical contacts.

Signal to noise ratio drops as the sliding distance rises from 1 km to 3 km. This suggests that wear will decrease more over longer distances because wear accumulates over longer contact times and distances.

Rao et al. [41] used liquid metallurgy to produce Al-Si/SiC alloy composite and examined its dry sliding wear behavior. In comparison to the Al-Si alloy, the composite exhibited a slightly lower friction coefficient and lower wear loss, as per the experimental results, which were conducted by varying the applied load at a constant velocity. Singh et al. [42] investigated the wear of Al-MMCs, particularly AA6082-T6 reinforced with SiC and B_4C particles. Response surface methodology was adopted to optimize the following important parameters: load, sliding distance, sliding speed, and percentage of reinforcement weight. Sliding distance, followed by sliding speed, load, and reinforcement loading, was found to have the greatest impact on wear for both composites. Vetrivel and colleagues [43] investigated the wear of AlSi7Mg composite samples reinforced with a hybrid composite of graphite and tungsten carbide particles. The wear behavior also showed a similar trend. Together, these studies demonstrate that the composite structure, load, sliding parameters, and type of reinforcement all have a substantial impact on the mechanical performance and wear resistance of Al-based MMCs.

3.5 Signal-to-Noise ratio analysis

The software "Minitab Release 21" was used to obtain SN ratios for their corresponding experimental wear loss values in order to create the SN ratio response table. Using the delta value, the parameter's influence was ascertained. The delta value is the difference between the parameter's highest and lowest SN ratios. A greater influence parameter is indicated by a higher delta value.

Table 9. Response table for SN ratios.

Levels	SiC wt. % (A)	Applied load (B)	Speed (C)	Distance (D)
1	42.95	45.20	45.50	45.19
2	44.09	44.13	43.76	44.08
3	45.42	43.13	43.21	43.19
Delta	2.47	2.07	2.29	2.00
Rank	1	3	2	4

The order of the parameters that affect wear loss, including wt. % of SiC (A), sliding speed (C), applied normal load (B), and sliding distance (D), is displayed in Table 9. It is clear from Table 9 that the wt. % of SiC is the most significant factor results, which demonstrated that each factor played a role in the wear loss all Cu/SiC composites. When compared to (C), (B), and (D). Table 10 demonstrates the significance of the ANOVA.

Table 10. ANOVA table for wear loss of Cu/SiC composites.

Source	DF-	Seq SS	Adj SS	Adj MS	F - Value-	P	% contribution
SiC wt. % (A)	2	27.445	27.445	13.7227	83.76	0.0000	29.33
Applied load (B)	2	19.331	19.331	9.6657	58.99	0.0000	20.66
Sliding speed (C)	2	25.758	25.758	12.8788	78.22	0.0000	27.53
Sliding distance (D)	2	18.077	18.077	9.0386	52.40	0.0000	19.32
Error-	18	2.949	2.949	0.1638			3.15
Total-	26	93.561					100.00

Abbreviation: DF–Degrees of freedom, Seq SS–Sequential sum of squares, Adj SS–Adjacent sum of squares, Adj MS–Adjacent mean squares, R^2 = 96.8% R^2adj = 95.4%

3.6 Analysis of variance for wear loss

Contributions were split by each parameter using ANOVA, which was then used to examine the overall variability of SN ratios. The sum of squares deviation to total sum of squares ratio was used to calculate parameter variability. A 95 % confidence level was used for the analysis. Wear behavior is significantly influenced by parameters with P-values less than 0.05.

Based on four factors, the statistical analysis of wear loss in Cu/SiC composites is shown in this ANOVA Table 10. The percentage contributions of the factors are as follows: With the largest contribution (29.33 %), SiC loading (A) has the greatest effect on wear loss. Other significant contributors include sliding speed (C) (27.53 %) and applied load (B) (20.66 %). The contribution of sliding distance (D) is 19.32 %, suggesting a significant but marginally diminished effect. Only 3.15 % of the variation in wear loss can be explained by the error, indicating that the model largely explains the variation. In conclusion, all four factors have a significant impact on Cu/SiC composite wear loss, with SiC loading having the greatest influence. A model that fits well and produces dependable results is suggested by the low error percentage.

The wear loss (W_L), which was determined using the multiple linear regression method, is related to the control factors A, B, C, and D as follows:

$$W_L = 3.96 \times 10^{-3} - 0.176 \times 10^{-3} \times A + 0.069 \times 10^{-3} \times B + 0.004 \times 10^{-3} \times C + 0.639 \times 10^{-3} \times D \quad (3)$$

3.7 Contour plots

The contour plots in Figure 7 represent the effect of SiC wt. % on wear loss under different wear parameters: applied load, speed, and sliding distance. The ANOVA Table 10 (previously analyzed) quantifies these effects statistically. An explanation that incorporates both sets of evidence can be found as follows.

The effect of applied load vs. SiC wt. % is shown in Figure 7a. The contour plot shows that wear loss increases with higher applied load but decreases as SiC wt. % increases. The evidence from ANOVA Table 10 indicates that the applied load (B) accounts for 20.66% of the total wear loss, demonstrating that it plays a crucial role in the wear behavior of the composite. A higher applied load leads to increased material removal, confirming its significant impact on wear performance. Additionally, the SiC loading (A) contributes 29.33% to wear resistance, highlighting its effectiveness in reducing wear. This suggests that an increased SiC content enhances the composite's durability by improving hardness and wear resistance, thereby mitigating material loss during testing.

Figure 7b illustrates the relationship between sliding speed and SiC wt. %. Wear loss decreases as SiC wt. % increases but increases at higher sliding speeds. Sliding speed has a significant impact, as evidenced by ANOVA Table 10, which shows that it contributes 27.53 % to wear loss. Once more, wear is decreased by SiC loading (29.33 %), demonstrating the composite's ability to reduce wear at higher speeds.

Figure 7c illustrates the relationship between sliding distance and SiC wt. %. Wear loss rises with sliding distance (km) but falls as SiC wt. % rises. According to the data in ANOVA Table 10, the sliding distance accounts for 19.32 % of wear loss. Even over longer distances, wear loss is decreased by increasing SiC, as the plot illustrates. Thus, the conclusion that SiC improves wear resistance in Cu composites is strongly supported by both statistical (ANOVA) and graphical (contour plot) evidence.

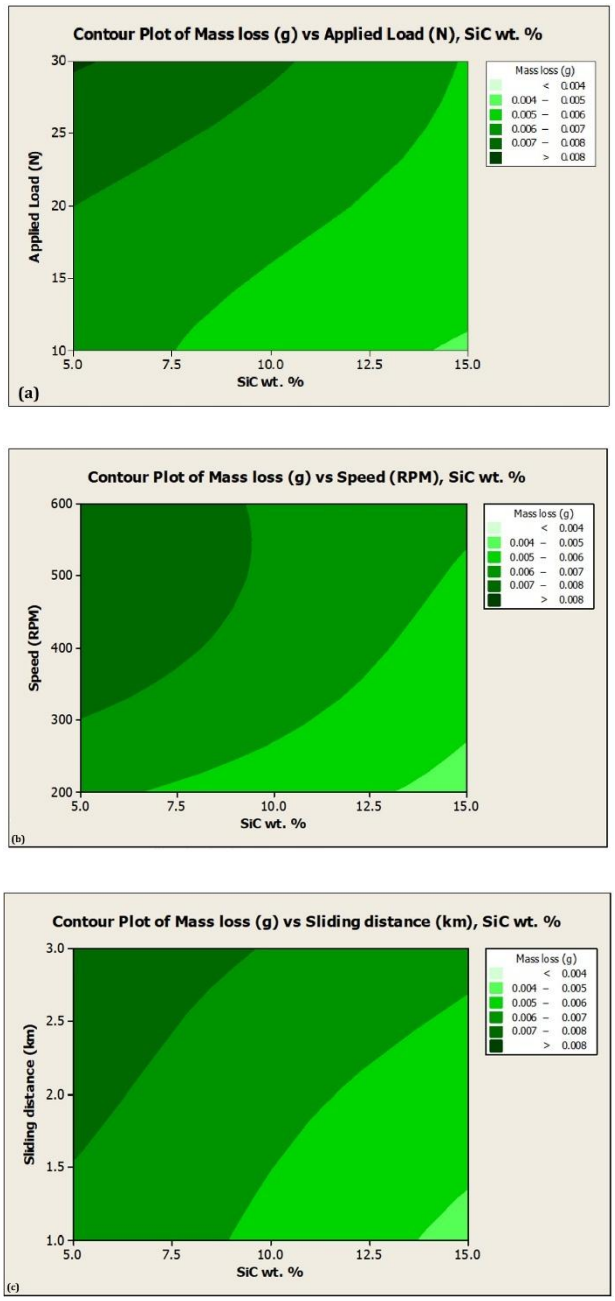

Fig. 7. Contour plot: (a) Applied load vs. SiC, (b) Speed vs. SiC, (c) Sliding distance vs. SiC.

3.8 Interaction plot analysis

Figure 8 displays the interaction plot for SN ratios, which shows how various factors interact and affect the response variable. Different factor levels and their effects on the response are represented by several lines in the plot. SN ratios are typically decreased by increasing SiC wt. % (A), applied load (B), sliding speed (C), and sliding distance (D). The differences in slopes and interactions show that the factor combinations have distinct effects on the response.

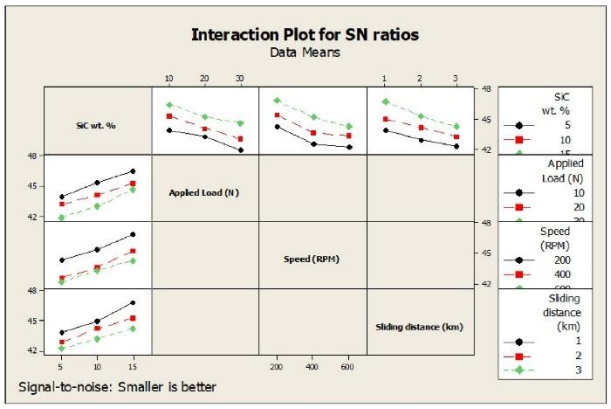

Fig. 8. Interaction plot for SN ratios.

The relationship between SiC wt. % (A) and applied load (B) is such that for all SiC wt. % levels, the SN ratio falls as the applied load rises. It appears that SiC loading affects the effect of applied load because the rate at which the SN ratio decreases varies slightly depending on the SiC wt. % level. For all SiC wt. % levels, the SN ratio decreases as speed increases due to the interaction between SiC wt % (A) and speed (C). A moderate interaction is indicated by the slightly different line slopes, which also imply that the SiC loading influences how speed affects the response. All SiC levels exhibit a decrease in SN ratios as sliding distance increases due to the interaction between SiC wt. % (A) and sliding distance (D). The interaction is evident from the different line slopes, which show that the wear behavior varies with varying sliding distances and SiC wt. %.

The SN ratio does, however, decrease with increasing speed, though the rate of decrease varies depending on the applied load (B) and speed (C). There is a discernible interaction, indicating that the combination of these two factors influences wear resistance. A similar pattern is seen in the interaction between sliding distance (D) and applied load (B) as sliding distance increases, the SN ratio decreases for all applied loads. SN ratios decrease as both speed and sliding distance increase, in line with the interaction between speed (C) and sliding distance (D).

3.9 Confirmation test

Confirmation testing is the last stage of the design process. To validate the statistical analysis, a dry sliding wear test was performed in this work using a combination of levels and parameters. In addition to validating the conclusions reached during the analysis phase,

the analytical methods indicate that the preferred combination of the factors' levels is significant. The test parameters for performing the dry sliding wear test are displayed in Table 11 (Sl. No.10 and 19 from Table 8). Following a confirmation experiment, the comparison of calculated and experimental values reveals an error related to dry sliding wear of composites that ranges from 0.324 % to 4.12 %.

Table 11. Confirmation tests results.

Level No.	Experimental weight loss (g)	Regression model weight loss (g)	Error (%)
10	0.0041	0.004269	4.122
19	0.0034	0.003389	0.324

3.10 Worn surface morphology

Worn surface of composite samples examinations were conducted under test conditions of 30 N applied load, 600 rpm sliding speed, and a 2 km sliding distance. The worn-out surfaces of the Cu/5SiC composite (Fig. 9a) exhibits the formation of irregular pits and broad abrasive grooves. In contrast to pits, which are indicative of ductile fracture, grooves show the counter surface micro-cutting effect. Delamination is not seen in this instance.

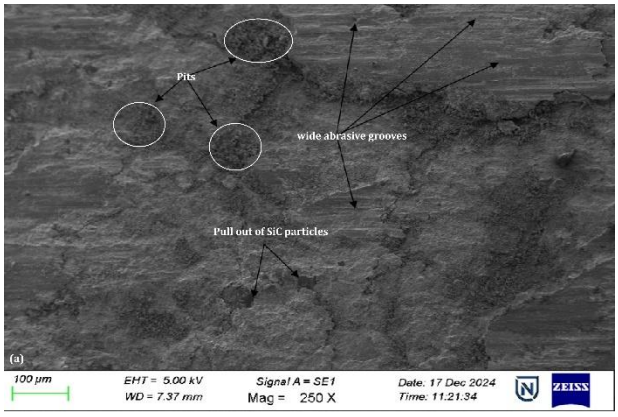

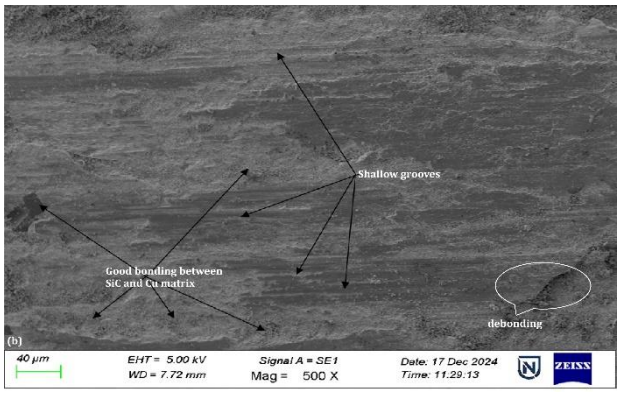

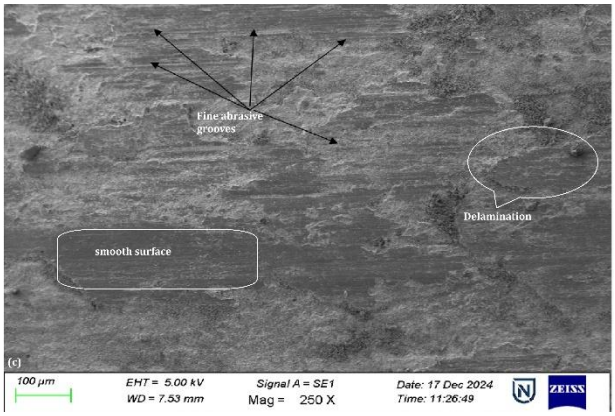

Fig. 9. Worn-out surfaces of: (a) Cu/5SiC, (b) Cu/10 SiC, (c) Cu/15SiC.

For the Cu composite with 10 wt. % SiC particles, shallow abrasive grooves are visible in the sliding direction in contrast to the worn-out surface of the Cu/ 5 wt. % SiC sample (Fig. 9b). The wear mechanism transitioned from a severe to a mild form.

The worn-out surface of a Cu composite with 15 wt. % SiC particles dispersed throughout it is shown in Figure 9c. The wear test revealed a smooth surface with thin abrasive grooves, indicating very little wear loss and mild wear. Therefore, it can be said that the wear in the 5 wt. % SiC-reinforced Cu sample has changed from being of the severe type. The primary wear mechanism characteristic observed in all Cu/SiC composites is abrasive wear. Thus, it can be concluded that adding SiC particles increases copper's resistance to wear.

4. CONCLUSION

The objective of this study is to determine the optimal method for producing a composite material with enhanced wear resistance, making it suitable for brake pads and bearings. The influence of SiC loading on the dry sliding wear performance of Cu matrix composites was analyzed. Taguchi's experimental design incorporated several control factors, including SiC wt. %, applied load, sliding speed, and sliding distance. The key findings are as follows.

- The study effectively demonstrated the use of the powder metallurgy technique to produce Cu/SiC composites. Microstructural analysis revealed a uniform and homogeneous dispersion of SiC particles within the Cu

matrix across all composite samples. The consistent distribution in all Cu/SiC composites underscores the efficiency of the powder metallurgy technique in fabricating high-quality MMCs.

- The Cu/15SiC composites exhibit a significantly higher hardness (23.8% greater than pure Cu), primarily due to the inherent hardness of SiC, which arises from its strong covalent and ionic bonds.
- Minimizing wear loss requires optimizing the material composition by increasing SiC loading. The improved hardness and wear resistance provided by SiC particles contribute to this enhancement. Increasing SiC from 5 to 10 wt. % led to a 15.73 % reduction in wear loss, whereas an increase from 10 to 15 wt. % resulted in a 9.33 % decrease in wear loss.
- The response table to S/N ratios indicate that the wt. % of SiC (A; delta value 2.47), is the most influential factor affecting wear loss, followed by sliding speed (C), applied load (B), and sliding distance (D).
- The ANOVA analysis highlights SiC wt. % (A) as the primary factor influencing wear behavior, accounting for 29.33 % of the variance in output responses. In comparison, the contributions of sliding speed (C), applied load (B), and sliding distance (D) are 27.53 %, 20.66 %, and 19.32 %, respectively.
- As SiC loading increases, the wear mechanism shifts from severe to mild, with higher SiC content resulting in shallower abrasive grooves and reduced wear loss. Notably, the Cu composite reinforced with 15 wt. % SiC exhibited the best wear resistance, characterized by thin abrasive grooves and a smoother surface.
- The findings of this research have significant implications for industries requiring materials with enhanced wear resistance, including applications in bearings and brake pads. Additionally, these composites are beneficial in electrical applications such as sliding contacts, where durability and conductivity rely on wear resistance. Further research on optimizing SiC particle size (micro to nano), corrosion resistance, life cycle, and cost analysis will unlock the full potential of Cu/SiC composites, making them a versatile solution for various wear-critical engineering challenges.

Acknowledgement

I would like to express my sincere gratitude to Jain Institute of Technology, Davangere, Karnataka, and Smt. Kamala and Sri Venkappa M. Agadi College of Engineering & Technology, Lakshmeshwar, for providing the research facilities that enabled the successful completion of this work.

REFERENCES

[1] N. B. Dhokey and R. K. Paretkar, "Study of wear mechanisms in copper-based SiCp (20% by volume) reinforced composite," *Wear*, vol. 265, no. 1–2, pp. 117–133, Dec. 2007, doi: 10.1016/j.wear.2007.09.001.

[2] S. C. Tjong and K. C. Lau, "Abrasive wear behavior of TiB2 particle-reinforced copper matrix composites," *Materials Science and Engineering A*, vol. 282, no. 1–2, pp. 183–186, Apr. 2000, doi: 10.1016/S0921-5093(99)00752-2.

[3] J. He, N. Zhao, C. Shi, X. Du, J. Li, and P. Nash, "Reinforcing copper matrix composites through molecular-level mixing of functionalized nanodiamond by co-deposition route," *Materials Science and Engineering A*, vol. 490, no. 1–2, pp. 293–299, Jan. 2008, doi: 10.1016/j.msea.2008.01.046.

[4] Y. Zhan and G. Zhang, "The effect of interfacial modifying on the mechanical and wear properties of SiCp/Cu composites," *Materials Letters*, vol. 57, no. 29, pp. 4583–4591, May 2003, doi: 10.1016/S0167-577X(03)00365-3.

[5] G. C. Efe, M. Ipek, S. Zeytin, and C. Bindal, "An investigation of the effect of SiC particle size on Cu–SiC composites," *Composites Part B Engineering*, vol. 43, no. 4, pp. 1813–1822, Jan. 2012, doi: 10.1016/j.compositesb.2012.01.006.

[6] J. Freudenberger and H. Warlimont, "Copper and Copper alloys," in Springer handbooks, 2018, pp. 297–305. doi: 10.1007/978-3-319-69743-7_12.

[7] R. Zhang, L. Gao, and J. Guo, "Effect of Cu2O on the fabrication of SiCp/Cu nanocomposites using coated particles and conventional sintering," *Composites Part a Applied Science and Manufacturing*, vol. 35, no. 11, pp. 1301–1305, Jul. 2004, doi: 10.1016/j.compositesa.2004.03.021.

[8] G. Celebi_Efe, I. Altinsoy, M. Ipek, S. Zeytin, and C. Bindal, "Some properties of Cu-SiC composites produced by powder metallurgy method," *Kovove Materialy-Metallic Materials*, vol. 49, no. 2, pp. 131–136, Jan. 2011, doi: 10.4149/km_2011_2_131.

[9] J. Zhu, L. Liu, H. Zhao, B. Shen, and W. Hu, "Microstructure and performance of electroformed Cu/nano-SiC composite," *Materials & Design (1980-2015)*, vol. 28, no. 6, pp. 1958–1962, Jun. 2006, doi: 10.1016/j.matdes.2006.04.021.

[10] G. Celebi Efe, T. Yener, I. Altinsoy, M. Ipek, S. Zeytin, "The fabrication and properties of SiC particulate reinforced copper matrix composites," in: 13th International materials symposium, Denizli, Turkey, 2010.

[11] J. S. Kim, D. H. Kwon, T.D. Nguyen, K. H. Huynh, P. P. Choi, M. G. Chang, Y. J. Yum and Y. S. Kwon, "Mechanical, electrical and wear properties of Cu-TiB_2 nanocomposites fabricated by MA-SHS and SPS," *Journal of Ceramic Processing Research*, vol. 7, no. 3 ,pp. 275-279, 2006.

[12] A. Vencl, A. Rac, and I. Bobić, "Tribological behaviour of Al-based MMCs and their application in automotive industry," *Tribology in Industry*, vol. 26, no. 3-4, pp. 3-38, 2004.

[13] K. Suryanarayanan, R. Praveen, and R. S., "Silicon Carbide Reinforced Aluminium Metal Matrix Composites for Aerospace Applications: A Literature Review," *International Journal of Innovative Research in Science*, Engineering and Technology, vol. 2, n0. 11, pp. 6336-6344, 2013.

[14] M. R. Rahimipour, A. A. Tofigh, M. O. Shabani, and P. Davami, "The enhancement of wear properties of compo-cast A356 composites reinforced with Al_2O_3 nano particulates," *Tribology in Industry*, vol. 36, no. 2, pp. 220-227, 2014.

[15] A. M. Sankhla *et al.*, "Effect of mixing method and particle size on hardness and compressive strength of aluminium based metal matrix composite prepared through powder metallurgy route," *Journal of Materials Research and Technology*, vol. 18, pp. 282–292, Feb. 2022, doi: 10.1016/j.jmrt.2022.02.094.

[16] K. K. Alanemea and T. M. Adewalea, "Influence of rice husk ash - Silicon carbide weight ratios on the mechanical behaviour of Al-Mg-Si alloy matrix hybrid composites," *Tribology in Industry*, vol. 35, no. 2, pp. 163- 172, 2013.

[17] J. Kumar *et al.*, "Investigation on the mechanical, tribological, morphological and machinability behavior of stir-casted Al/SiC/Mo reinforced MMCs," *Journal of Materials Research and Technology*, vol. 12, pp. 930–946, Mar. 2021, doi: 10.1016/j.jmrt.2021.03.034.

[18] Y. Wang and T. Monetta, "Systematic study of preparation technology, microstructure characteristics and mechanical behaviors for SiC particle-reinforced metal matrix composites," *Journal of Materials Research and Technology*, vol. 25, pp. 7470–7497, Jul. 2023, doi: 10.1016/j.jmrt.2023.07.145.

[19] M. Shabani, M. H. Paydar, R. Zamiri, M. Goodarzi, and M. M. Moshksar, "Microstructural and sliding wear behavior of SiC-particle reinforced copper matrix composites fabricated by sintering and sinter-forging processes," *Journal of Materials Research and Technology*, vol. 5, no. 1, pp. 5–12, Apr. 2015, doi: 10.1016/j.jmrt.2015.03.002.

[20] S. C. Tjong and K. C. Lau, "Tribological behaviour of SiC particle-reinforced copper matrix composites," *Materials Letters*, vol. 43, no. 5–6, pp. 274–280, May 2000, doi: 10.1016/S0167-577X(99)00273-6.

[21] T. R. Bement, "Taguchi Techniques for Quality Engineering," *Technometrics*, vol. 31, no. 2, pp. 253–255, May 1989, doi: 10.1080/00401706.1989.10488519.

[22] G. Taguchi and V. Cariapa, *Taguchi on robust technology development*. 1993. doi: 10.1115/1.800288.

[23] Y. Sahin, "Tribological behaviour of metal matrix and its composite," *Materials & Design (1980-2015)*, vol. 28, no. 4, pp. 1348–1352, Apr. 2006, doi: 10.1016/j.matdes.2006.01.032.

[24] S. Suresha and B. K. Sridhara, "Effect of addition of graphite particulates on the wear behaviour in aluminium–silicon carbide–graphite composites," *Materials & Design (1980-2015)*, vol. 31, no. 4, pp. 1804–1812, Nov. 2009, doi: 10.1016/j.matdes.2009.11.015.

[25] M. R. Akbarpour *et al.*, "An overview of friction stir processing of Cu–SiC composites: Microstructural, mechanical, tribological, and electrical properties," *Journal of Materials Research and Technology*, vol. 27, pp. 1317–1349, Sep. 2023, doi: 10.1016/j.jmrt.2023.09.200.

[26] Y. Zhan and G. Zhang, "Friction and Wear Behavior of Copper Matrix Composites Reinforced with SiC and Graphite Particles," *Tribology Letters*, vol. 17, no. 1, pp. 91–98, Feb. 2004, doi: 10.1023/B:TRIL.0000017423.70725.1c.

[27] S. Bai *et al.*, "Enhanced tribological, electrical, and thermal properties of SiC/Cu composites by SiO2–Cu2O glass phase modification," *Ceramics International*, vol. 50, no. 1, pp. 750–756, Oct. 2023, 2024, doi: 10.1016/j.ceramint.2023.10.153.

[28] Akbarpour, F. G. Asl, H. M. Mirabad, and H. S. Kim, "Microstructural characterization and enhanced tensile and tribological properties of Cu–SiC nanocomposites developed by high-pressure torsion," *Journal of Materials Research and Technology*, vol. 20, pp. 4038–4051, Sep. 2022, doi: 10.1016/j.jmrt.2022.08.141.

[29] X. Cao, J. Duan, C. Wang, P. Jin, Y. Yang, and J. Zhang, "Structure design and tribological properties of Cu–SiC foam ceramic composites," *Ceramics International*, vol. 50, no. 5, pp. 7366–7373, Dec. 2023, doi: 10.1016/j.ceramint.2023.11.383.

[30] M. R. Akbarpour *et al.*, "Recent advances in processing, and mechanical, thermal and electrical properties of Cu-SiC metal matrix composites prepared by powder metallurgy," *Progress in Materials Science*, vol. 140, p. 101191, Sep. 2023, doi: 10.1016/j.pmatsci.2023.101191.

[31] M. A. Metwally, M. M. Sadawy, M. Ghanem, and I. G. E.- Batanony, "The role of Nano-SIC on microstructure and tribo-logical properties of SIC/CU Nano-Composite," *Journal of Engineering Research and Reports*, pp. 35–44, Aug. 2020, doi: 10.9734/jerr/2020/v15i417153.

[32] C. Shekhar, M. F. Wani, R. Sehgal, S. S. Saleem, U. Ziyamukhamedova, and N. Tursunov, "Recent progress in Particulate Reinforced Copper-Based Composites: Fabrication, Microstructure, Mechanical, and Tribological Properties—A review," *Advanced Engineering Materials*, Dec. 2024, doi: 10.1002/adem.202401748.

[33] ASTM E18/18M-11, Standard Test Methods for Rockwell Hardness of Metallic Materials, ASTM International, 2018.

[34] ASTM G99-17, Standard test method for wear testing with a pin-on-disk apparatus, ASTM International, 2017.

[35] T. K. R. S, P. Narayanasamy, A. N. Balaji, and S. C. Vettivel, "Microstructural, electrical, thermal and tribological studies of copper-fly ash composites through powder metallurgy," *DOAJ (DOAJ: Directory of Open Access Journals)*, Dec. 2018, doi: 10.24425/bpas.2018.125941.

[36] N. Somani, Y. K. Tyagi, P. Kumar, V. Srivastava, and H. Bhowmick, "Enhanced tribological properties of SiC reinforced copper metal matrix composites," *Materials Research Express*, vol. 6, no. 1, p. 016549, Oct. 2018, doi: 10.1088/2053-1591/aae6dc.

[37] K. Bandil *et al.*, "Microstructural, mechanical and corrosion behaviour of Al–Si alloy reinforced with SiC metal matrix composite," *Journal of Composite Materials*, vol. 53, no. 28–30, pp. 4215–4223, Jun. 2019, doi: 10.1177/0021998319856679.

[38] M. K. Abbass and N. A. B. Sharhan, "Characteristics of AL6061-SIC-AL2O3 surface hybrid composites fabricated by friction stir processing," *Journal of Materials and Engineering*, vol. 1, no. 4, pp. 147–158, Jan. 2023, doi: 10.61552/jme.2023.04.002.

[39] A. K. MS, "Evaluation of Tribological Properties of Aluminium-SIC-B4C Hybrid Composites pages 229-234," *Journal of Materials and Engineering*, vol. 2, no. 3, pp. 229–234, Jun. 2024, doi: 10.61552/jme.2024.03.008.

[40] C. Ayyappadas, A. R. Annamalai, D. K. Agrawal, and A. Muthuchamy, "Conventional and microwave assisted sintering of copper-silicon carbide metal matrix composites: a comparison," *Metallurgical Research & Technology*, vol. 114, no. 5, p. 506, Jan. 2017, doi: 10.1051/metal/2017033.

[41] R. N. Rao, S. Das, and P. V. Krishna, "Experimental investigation on the influence of SiC particulate reinforcement in aluminium alloy composites," *Proceedings of the Institution of Mechanical Engineers Part J Journal of Engineering Tribology*, vol. 222, no. 1, pp. 1–6, Jan. 2008, doi: 10.1243/13506501JET333.

[42] G. Singh, S. Goyal, G. Miranda, and N. Sharma, "Parametric study of the dry sliding wear behaviour of AA6082-T6/SiC and AA6082-T6/B4C composites using RSM," *Journal of Mechanical Science and Technology*, vol. 32, no. 2, pp. 579–592, Feb. 2018, doi: 10.1007/s12206-018-0105-5.

[43] K. P. Vetrivel, R. Subramanian, and K. S. Vinoth, "Influence of Wear Parameters on Dry Sliding Wear Behaviour of Al Alloy Hybrid Composites Using Taguchi Method," *Advances in Natural and Applied Sciences*, vol. 10, no. 6 SE, pp. 52-67, 2016.